Proc. Natl. Acad. Sci. USA
Vol. 80, pp. 741–744, February 1983
Biophysics

X-ray scattering from the superhelix in circular DNA

(supercoiling/diffraction from solutions/specific linking difference/writhe vs. twist)

G. W. BRADY*, D. B. FEIN*, H. LAMBERTSON†, V. GRASSIAN†, D. FOOS†, AND C. J. BENHAM‡

*Center for Laboratories and Research, New York State Department of Health, Albany, New York 12222; †Rensselaer Polytechnic Institute, Troy, New York 12181; and ‡Department of Mathematics, University of Kentucky, Lexington, Kentucky 40506

Communicated by Bruno H. Zimm, October 25, 1982

ABSTRACT **This communication presents measurements, made with a newly constructed position-sensitive detector, of the small-angle x-ray scattering from the first-order superhelix of native COP608 plasmid DNA. This instrument measures intensities free of slit effects and provides good resolution in the region of interest. The reported observations, made both in the presence and in the absence of intercalator, closely fit the scattering patterns calculated for noninterwound helical first-order superhelices. These results are consistent with a toroidal helical structure but not with interwound conformations. The pitch angle α and contour length per turn c are reported for the native molecule at several concentrations of the platinum intercalating compound. From these parameters, the best-fitting toroidal helix is constructed and its geometry is investigated. The specific linking difference of the native molecule is estimated to be $\Delta Lk/Lk_0 \approx -0.055$. If the best-fitting toroidal helix is taken to be the actual structure, the partitioning of superhelicity between twist and writhe occurs in the approximate ratio of 2:1.**

The large-scale tertiary structure of a covalently closed, circular DNA molecule (ccc DNA) in solution is known to be drastically affected by the internal stresses imposed by superhelicity. The variations of sedimentation velocity with increased supercoiling suggest a decreasing (average) radius of gyration as the molecule assumes more compact conformations (1). In addition to hydrodynamic methods, small-angle x-ray scattering (SAS) may be used to investigate large-scale properties of stressed DNA structure in solution. The observed scattering intensity is related to the distribution of electron pairs within the molecule and hence provides structural information.

Hydrodynamic evidence (2) indicates that dissolved superhelical polyoma ccc DNA may undergo an ionic strength-dependent transition between an interwound conformation (high salt) and a toroidal (super)helix ($Na^+ \simeq 0.01$ M). The interwound superhelical structure observed by electron microscopy may not be representative of solution conformations because the samples are spread flat and dried in preparation for photography. Previous communications (3, 4) reported the x-ray scattering from two natively superhelical ccc DNAs in solution, PM2 [≈10,600 base pairs (bp)] and PBR313 (≈4,400 bp). The observed superhelix diffraction patterns were consistent with a noninterwound coiled coil geometry, the first (i.e., smallest) order of which had a contour length of $c \simeq 920$ Å per turn at a pitch angle $45° < \alpha < 55°$. However, those results were presented as being preliminary in nature because practical limitations of the experiment precluded correcting the data for slit effects. The intensities in the region where the first-order scatters were measured with a Kratky camera having infinite slit geometry. Because of the low intensities involved, slit widths considerably greater than optimal had to be used. This decreased the lower angle limit of resolution of the instrument because the inner portion of the scattering curve was superimposed on a rising background resulting from parasitic slit scattering. In consequence, the resulting data could not be desmeared, so a direct comparison with theory was precluded.

This paper presents measurements of SAS from the first-order ccc DNA superhelix made with a new position-sensitive detector (PSD). The resulting profiles are free of slit effects, permitting direct and unambiguous comparisons with theory.

MATERIALS AND METHODS

The apparatus used will be described in detail elsewhere. Briefly, it consists of a beam powered by a Rigaku 12-kW rotating anode source operated at 50 kV and 190 mA collimated by two pinholes 0.75 mm in diameter set 100 cm apart in an evacuated collimation chamber. The beam irradiates the sample contained in a flat sample holder with mica windows separated by a path length of 1 mm. Its diffraction pattern is recorded on a PSD placed at the end of an evacuated path 150 cm from the sample. An extra guard pinhole, diameter 0.8 mm, is placed just before the sample. With this arrangement, the slit scattering is effectively reduced to an insignificant value everywhere but at the innermost region of the pattern. Because of the small size of the beam and the large sample-to-detector distance, slit corrections are not necessary. The intensity loss associated with the greatly increased collimation of the pinholes and the large scattering radius are adequately compensated for by the much greater power output of the 12-kW generator. Thus, we are now able to obtain direct traces of the diffraction patterns free of all corrections with the exception of a fairly minor one due to the finite width of the main beam. This causes an overlap of two or three channels of the PSD and is not significant.

In these experiments the DNA used was the natively supercoiled COP608 plasmid (4,258 bp), a 179-bp deletion of the PT 181 plasmid of *Staphylococcus aureus*. The cells were grown overnight in Cy broth, harvested by centrifugation, and lysed by the clear lysate method (5). Purification of the superhelical DNA was done according to the acid/phenol extraction procedure of Zasloff *et al.* (6). The DNA solution was freed of RNA and protein impurities. The DNA was precipitated, resuspended in low ionic strength buffer, and then twice extracted with 1 vol of redistilled phenol equilibrated with 50 mM NaOAc to a pH of 4.0. As shown by Zasloff *et al.* (6), nicked and chromosomal DNA will be selectively removed from the aqueous phase by this process, leaving a 95% pure solution of superhelical DNA. The phenol was removed by ether extraction. The solution was ethanol precipitated and the DNA was resuspended in the buffer used for the x-ray experiments (0.2 M Tris·HCl, pH 7.5/0.05 M NaCl/1.0 mM Na_2EDTA). In certain

The publication costs of this article were defrayed in part by page charge payment. This article must therefore be hereby marked "*advertisement*" in accordance with 18 U. S. C. §1734 solely to indicate this fact.

Abbreviations: ccc DNA, covalently closed circular DNA; SAS, small-angle x-ray scattering; PSD, position-sensitive detector; bp, base pairs (bp); PtTS, 2-hydroxyethanethiolato(2,2′,2″,-terpyridine) platinum(II).

cases the appropriate concentration of the intercalating agent 2-hydroxyethanethiolato(2,2′,2″-terpyridine)platinum(II) (PtTS) was added. For comparison, calf thymus DNA (type I, Sigma) was dissolved in buffer (0.2 M Tris·HCl, pH 7.5/0.05 M NaCl/1 mM Na_2EDTA), ethanol precipitated, and dialyzed against the same buffer.

RESULTS AND ANALYSIS

Fig. 1 shows a plot of the superhelical scattering from a solution of plasmid COP608 DNA (11.6 mg/ml), M_r 2.8 × 10^6, along with the background scattering (lower curve) from the buffer solution (0.2 M Tris·HCl, pH 7.5/0.05 M NaCl/1 mM Na_2EDTA). Both curves are the actual output from the detector without smoothing. The counting time was 4 hr. Comparison of the two shows that the rapidly rising portion of the background is confined to channel numbers less than 52. Beyond this it levels off to a smoothly decreasing curve of very favorable signal-to-background ratio which can be averaged over a 5-channel interval by a least squares program and then directly subtracted from the DNA curves.

Fig. 2 shows the scattering curves, corrected for background, of calf thymus DNA (curve 1), of superhelical DNA (curve 2), and of superhelical DNA (curves 3, 4, and 5) in which PtTS had been intercalated in the mol ratios of 0, 1:30, 1:25 and 1:20 (mol PtTS intercalated/mol bp). The calf thymus curve is completely featureless. In contrast, the superhelical curves show pronounced maxima which decrease in magnitude with increasing PtTS/DNA ratios. This shows that the diffraction maxima are attributable to the superhelical conformation of the circular plasmid DNA. Curves taken at lower concentrations reproduce this behavior, so intermolecular scattering plays no part. The maximum for the nonintercalated DNA is particularly pronounced. Intercalation results in displacement of the curves out to larger s values, consistent with a decrease in contour length per turn, c, of the unwinding superhelix. (This latter effect will be demonstrated below, where the measured curves are compared with those calculated for both interwound and noninterwound helical supercoils.) The scatter in the data points could be smoothed out by using longer counting times. However, this risks nicking the DNA, with consequent relaxation of the superhelix. For the irradiation times used in the experiments of Fig. 2, no significant change was observed between the microdensitometer traces of the gel electrophoresis patterns after and before the intensities were measured, so nicking effects were minimal.

The scattering intensity from a population of identical, randomly oriented filaments may be calculated by using Debye's

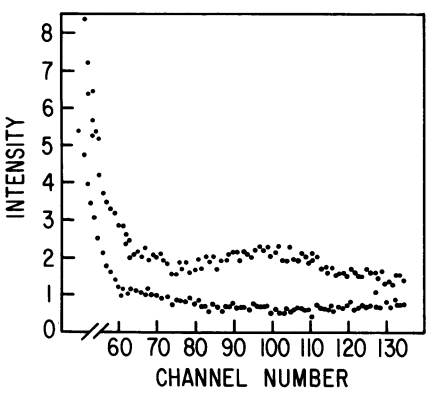

FIG. 1. Scattering (upper curve) and background (lower curve) curves of the DNA superhelix. The points are the output from the PSD. Counting time, 4 hr; DNA concentration, 11.6 mg/ml.

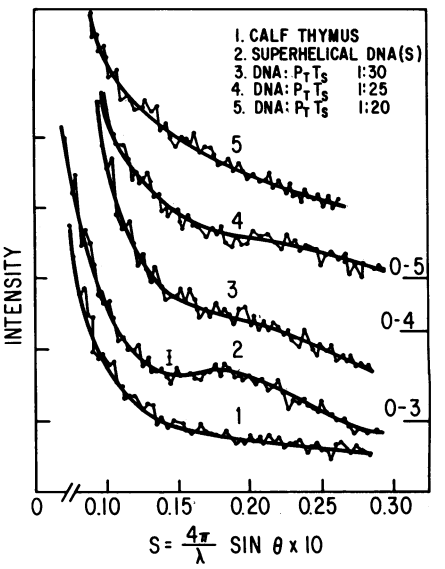

FIG. 2. Scattering curves (corrected for background) of calf thymus DNA and superhelical DNA at various intercalator ratios. The abscissa origins for curves 3 and 4 have been displaced upward. Concentrations and counting times were as in Fig. 1. The heavy continuous lines are calculated curves for noninterwound molecules.

equation (4, 7, 8)

$$I(s) = \frac{\rho^2}{2}\int_0^L dl_1 \int_0^L \frac{\sin sr(l_1,l_2)}{sr(l_1,l_2)}\, dl_2. \qquad [1]$$

Here, l_1 and l_2 are two copies of the length parameter, ρ is the effective electron density of the filament, and $s = 4\pi/\lambda \sin\theta$; λ is the wavelength (CuKα, λ = 1.54 Å) and θ is one-half the scattering angle. The variable r (l_1, l_2) is the distance in space between two points on the scattering filament and L is the filament length. If the supercoils are helical, their scattering may be computed by reducing Debye's equation to a one-variable expression which is integrated numerically (4). The scattering profiles of helically interwound (supercoiled) structures may be found in a similar manner. The dominant contribution to the scattering from interwound conformations comes from the relatively high density of electron pairs separated by distances near the interstrand separation. This remains true regardless of the pitch angle α of the interwound helix. In contrast, a noninterwound helical structure scatters in a manner strongly dependent on pitch angle (4).

Calculated curves may be fitted directly to the experimentally measured profiles (4). For noninterwound helical structures the shape of the calculated curve which best fits the experimental curve determines the pitch angle α on the corresponding helix; the angular scale at which scattering occurs is inversely related to the scale of the helix. It follows that the pitch angle α and contour length per turn, c, of the best-fitting helix may be found from the experimentally measured profiles, as has been shown (4). The calculated (noninterwound) scattering curves which best fit the present observations are shown as the solid lines in Fig. 2. The agreement between experiment and calculation is close in all cases. The resulting values of α and c are given in Table 1. From these quantities the radius r and pitch p of the helix may be found. The number N of the helical turns of the given scale which the COP608 plasmid could contain is given by L/c.

The mean (± SD) contour length per turn for the natively supercoiled COP608 plasmid is found to be 1,020 ± 20 Å with a pitch angle of α = 60° ± 2°. These results refine the previ-

Table 1. Measured superhelix parameters

PtTS/DNA, mol/mol	c	α, degrees	r, Å	p, Å
0	1,020 ± 20	60 ± 2	141	511
1:30	816 ± 10	50 ± 2	100	524
1:25	764 ± 10	45 ± 3	87	531
1:20	728 ± 10	39 ± 3	73	563

c and α are given as mean ± SD.

ously published estimates made from smeared data on native PM2 and PBR313 DNAs (4). Although the molecular lengths (and probably the superhelix densities) differ, the corrections introduced involve increases of approximately 10–15% in both α and c.

The scattering from interwound structures is dominated by interstrand electron pair correlations, as manifested by strong maxima at positions corresponding to the strand separation. This is shown in Fig. 3 where the theoretical scattering curves are plotted for two forms of interwound structures (curves 2 and 3) as well as the experimental data on the nonintercalated COP608 molecule (curve 1). The strong interstrand scattering, a feature common to interwound structures of all pitch angles, is not present in the experimental curve. This strongly suggests that the native COP608 DNA is not interwound when in solution under the experimental conditions used.

These results support the toroidal helical model of supercoiled structure, a conformation that is predicted to occur at stressed elastic equilibrium (9, 10). One may construct for each superhelical case the best-fitting toroidal helix having the given values of pitch angle α, contour length per turn c, and number of turns per molecule N. The length of the central axis of this structure is then Np, where p is the pitch. In a toroidal helix, this central axis forms a circle whose radius R is $Np/2\pi$. Values deduced from the experimental results for the helical radius r, the axial radius R, and their ratio $\tau = r/R$ are given in Table 2. The writhing number (Wr) of a toroidal helix of N turns and $\tau = r/R$, also given, is calculated by the following expression, which is derived by application of Fuller's integral (11):

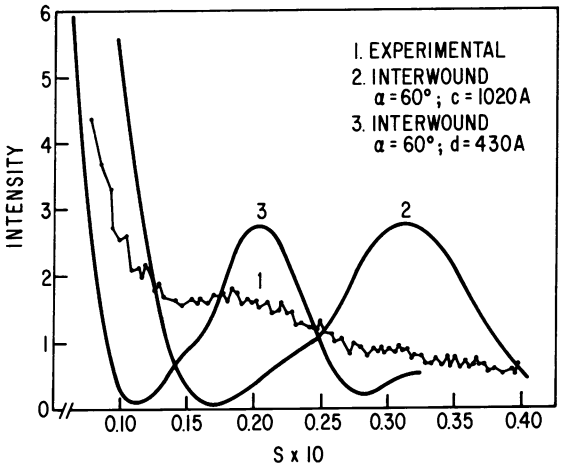

FIG. 3. Comparison of the experimental curve for the nonintercalated DNA with calculated curves for the two interwound configurations indicated in the legend.

density. In contrast, the ratio of radii $\tau = r/R$ is seen to decrease linearly with the absorbed undertwist ΔTw_I over the experimental range. The fit of these parameters to a regression line is extremely close ($r^2 = 0.996$).

Because the diffraction maxima become faint for angles of small pitch, determination of superhelix parameters is precluded when $\alpha < 30°$ (4). Unfortunately, this means that the range of experimental observations cannot be extended closer to the relaxed state. However, extrapolation of the phenomenological linear relationship between ΔTw_I and $\tau = r/R$ permits estimation of the amount of intercalatively absorbed twist that completely relaxes the molecule (i.e., $\tau = 0$). This occurs when $\Delta Tw_I = 22.4$, the x intercept of the regression line. Because the unstressed linking number of a molecule of $N = 4{,}258$ bp is $Lk_0 \approx 4{,}258/10.4$, one may estimate the specific linking difference of the native molecule under experimental conditions to be $\Delta Lk/Lk_0 \approx -22.4/409 = -0.055$. This value lies within the range of superhelicities found for other plasmids (13).

$$Wr(n,\tau) = \frac{-N}{2\pi}\int_0^{2\pi} \frac{\tau\cos N\theta\{[(1+\tau\cos N\theta)^2+\tau^2N^2]^{1/2}+(1+\tau\cos N\theta)\}+\tau^2N^2}{(1+\tau\cos N\theta)\{[(1+\tau\cos N\theta)^2+\tau^2N^2]^2+(1+\tau\cos N\theta)\}+\tau^2N^2}\,d\theta. \quad [2]$$

Here the variable of integration is θ, the angle subtended by an arc of the circular central axis. The values for Wr in Table 2 are for the best-fitting toroidal helices corresponding to the four superhelical curves of Fig. 2. Finally, each intercalation event unwinds the duplex by approximately 26° (12). Table 2 gives the average number of intercalated PtTS molecules in each DNA and the number of turns of undertwist, ΔTw_I, which are stabilized thereby.

The data given in the tables yield several important conclusions regarding superhelical structure and intercalative relaxation. First, both the pitch angle α and the contour length per turn c decrease as the molecule is relaxed. It follows that the number of turns N per molecule actually increases with intercalation, possibly due to the introduction of slight kinks. The simultaneous decrease of α and increase of N exert opposite influences on Wr. However, the data show that the magnitude of Wr for the best-fitting toroidal helix decreases with relaxation, in accord with the accepted mechanism of intercalation. However, the variations of Wr are not linear with intercalation

Finally, if the linking difference $\Delta Lk = Lk - Lk_0 = -22.4$ and Wr is -7.0, then the total molecular torsional deformation is $\Delta Tw = \Delta Lk - Wr = -15.4$. That is, the native molecule under experimental conditions is estimated to partition its superhelical deformation between twist and writhe in the approximate ratio of 2:1. This result is consistent with a previous estimate made by using a different method (14).

Table 2. Calculated properties*

PtTS/DNA, mol/mol	N	ΔTw_I	R, Å	r/R	Wr
0	14	0	1,139	0.124	7.01
1:30	18	10.25	1,480	0.0676	6.57
1:25	19	12.3	1,633	0.0572	5.57
1:20	20	15.4	1,792	0.0407	4.49

* For the parameters listed in Table 1, by using method described in the text. A toroidal conformation was assumed in computing the last three numbers.

DISCUSSION

The observations reported here show that, under the experimental conditions used, the superhelix does not occur in the interwound conformation. These results are consistent with the conclusions of Gray (2) whose hydrodynamic analysis suggests that superhelical polyoma ccc DNA occurs in a toroidal helical conformation at low ionic strength.

In addition to changes of large-scale tertiary structure, superhelical stresses could induce local conformational transitions to alternative secondary structures having different unstressed twist rates (14). It follows that the stressed behavior of any specific DNA molecule can be quite complex in practice. The present experimental techniques will do much to illuminate the interactions between large-scale tertiary structure and local secondary structure in a supercoiled molecule.

We acknowledge the assistance of Dr. Stephen Carleton of the Public Health Institute of New York City who kindly provided sufficient quantities of *S. aureus* cells for the extraction of the plasmid DNA, and the National Science Foundation for financial support (Grants PCM-8041337 supporting G.W.B. and PCM-8002814 supporting C.J.B.). In addition, C.J.B. was supported in part by an Alfred P. Sloan Fellowship.

1. Upholt, W., Gray, H. B. & Vinograd, J. (1971) *J. Mol. Biol.* **61**, 21–38.
2. Gray, N. B. (1967) *Biopolymers* **5**, 1009–1019.
3. Brady, G. W., Fein, D. B. & Brumberger, H. (1976) *Nature (London)* **264**, 231–234.
4. Benham, C. J., Brady, G. W. & Fein, D. B. (1980) *Biophys. J.* **29**, 351–366.
5. Novick, R. P. & Bouanchaud, D. (1971) *Ann. N.Y. Acad. Sci.* **182**, 279–294.
6. Zasloff, M., Ginder, G. D. & Felsenfeld, G. (1978) *Nucleic Acids Res.* **5**, 1139–1152.
7. Debye, P. (1915) *Ann. Physik* **46**, 809–824.
8. Schmidt, P. W. (1965) in *Small Angle X-Ray Scattering*, ed. Brumberger, H. (Gordon & Breach, New York), pp. 17–31.
9. Benham, C. J. (1977) *Proc. Natl. Acad. Sci. USA* **74**, 2397–2401.
10. Benham, C. J. (1979) *Biopolymers* **18**, 609–623.
11. Fuller, F. B. (1979) *Proc. Natl. Acad. Sci. USA* **78**, 3557–3561.
12. Wang, J. C. (1974) *J. Mol. Biol.* **89**, 738–801.
13. Bauer, W. R. (1978) *Annu. Rev. Biophys. Bioeng.* **7**, 287–313.
14. Benham, C. J. (1979) *Proc. Natl. Acad. Sci. USA* **76**, 3870–3874.